Suraj Rao, Shankho Ganguli, and Mark G. Rabbat

Introduction

Since the advent of multi-detector CT scanners, much progress has been made in the evaluation of peripheral arterial disease. Spiral CT was introduced in the early 1990s providing basic assessment of vasculature during contrast injection studies. However, it was multichannel CT that provided the resolution required to confidently elucidate vascular disease. Multi-slice CT emerged in the late 1990s and allowed for better volume coverage with shorter scan times, as multiple slices could be captured during one gantry rotation with decreased gantry rotation time. Overlapping image slices during reconstruction add to the improved longitudinal resolution, and post-processing techniques using submillimeter slices allow for superior two and three-dimensional rendering (Fig. 17.1). Table 17.1 provides a list of key terms to better understand the literature.

In a meta-analysis published in JAMA in 2009, 20 diagnostic cohort studies analyzed with 957 patients predominately presenting with intermittent claudication (68 %) showed that the overall sensitivity for CTA detecting more than 50 % stenosis or occlusion was 95 % (95 % CI, 92–97 %) and specificity was 96 % (95 % CI, 93–97 %), when compared to intra-arterial DSA [1] (Fig. 17.2). Understaging (underestimation of disease severity) occurred in 9 % of segments and overstaging (a significant stenosis was diagnosed by CTA as an occlusion) occurred in 4 % of segments. However, this meta-analysis only included one study with critical limb ischemia (CLI) patients, identifying the need for further evaluation in this population. In addition to lesion severity, CTA is also highly accurate in identifying length and number of lesions [2], as are required for correct treatment decisions per TASC guidelines, making CTA a valuable tool for therapeutic planning. More recent data with 64 slice CT scanning echoes previous studies, with 98 % accuracy for CT angiography detecting greater than 70 % stenosis, in a prospective cohort of 212 symptomatic PAD patients (acute CLI excluded) [3] (Fig. 17.3). It further suggested that results could be used to effectively guide clinical management, as therapy recommendations based on CT angiographic findings alone were identical to those based on DSA findings in all but one patient. Similar results can be found in a cohort of 41 patients with critical limb ischemia and severe claudication [4], making CTA a useful tool in treatment planning.

CT Angiogram: Protocol Basics

Typical CT angiography scanning protocols include a digital radiograph called the "scout image," a non-enhanced scan, a test bolus or bolus triggering, the contrast-enhanced CT angiogram, and an optional delayed-phase acquisition to capture late opacification of distal vessels. The delayed-phase acquisition may be necessary in conditions of slow moving contrast, due to severe vascular disease, low cardiac output states, or significant aneurysms. Popliteal artery aneurysms can be well visualized by CTA (Fig. 17.4).

Patients are positioned supine, arms overhead to reduce contributing artifact, and legs close together with slight internal rotation of the feet. Proper positioning is important. For example, plantar extension of the foot can cause compression of the popliteal artery by the gastrocnemius muscle in popliteal artery entrapment syndrome and can be misinterpreted as atherosclerotic steno-occlusive disease. Only a

S. Rao, MD
Department of Cardiology, Scripps, San Diego, CA, USA

S. Ganguli, MD
Cardiology, Aurora St. Luke's Medical Center,
Milwaukee, WI, USA

Cardiology, Aurora Sinai Medical Center, Milwaukee, WI, USA

M.G. Rabbat, MD (✉)
Department of Cardiology, Loyola University Chicago,
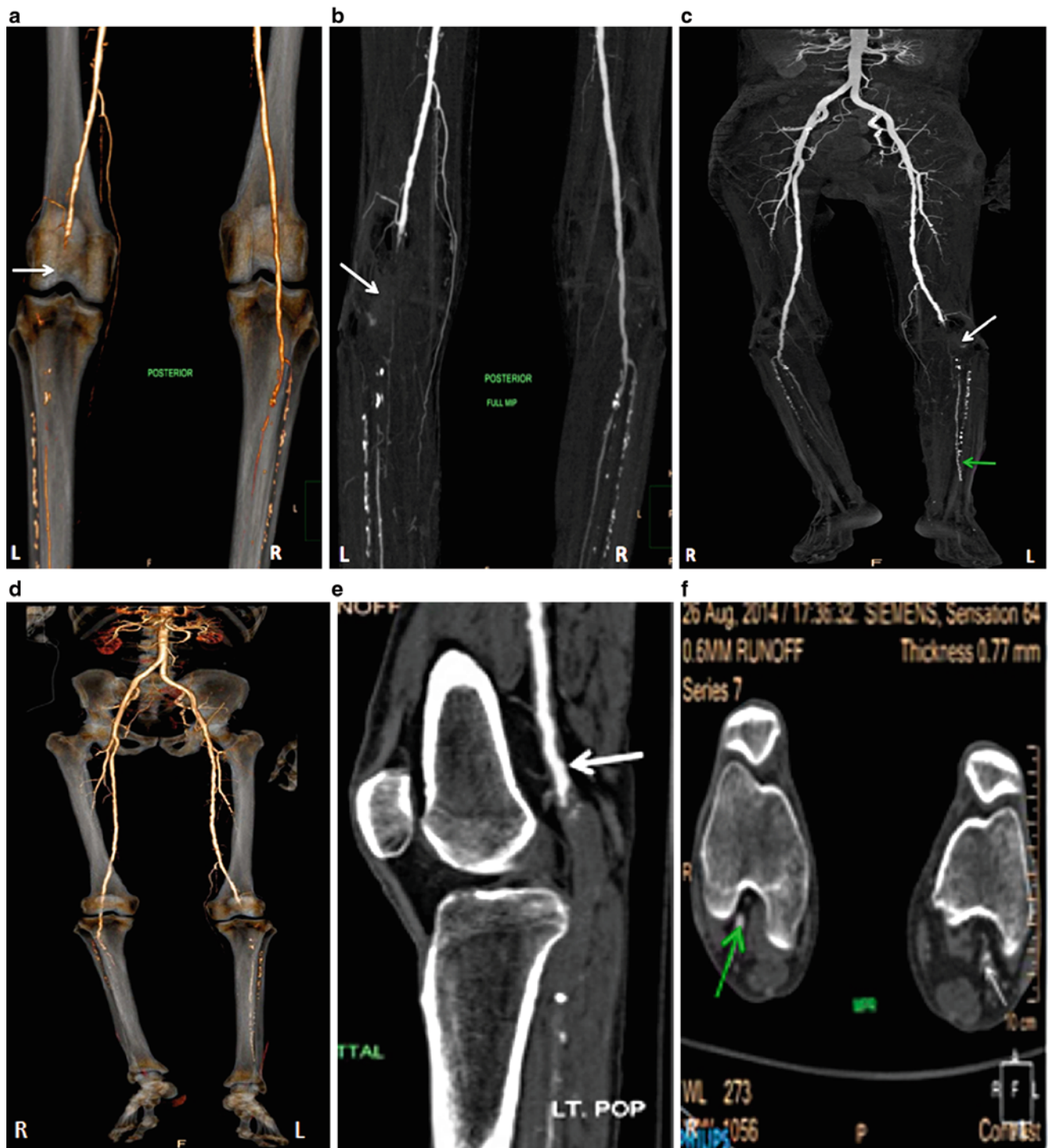2160 S. 1st Avenue, Building 110, Maywood, IL 60153, USA

Fig. 17.1 A 67-year-old male who presented, with LLE ischemic pain, found to have left popliteal artery occlusion, and seen in a–f. (**a**) Zoomed 3D VR with transparent bone for visual landmarks. (**b**) MIP, posterior view, with abrupt interruption of luminal enhancement at the L popliteal artery (*arrow*). (**c**) 3D full MIP showing L popliteal occlusion (*white arrow*) with faint distal reconstitution of the peroneal artery (*green arrow*) due to collateral flow. (**d**) 3D VR with transparent bone to better appreciate the vascular anatomy in relation to adjacent bony structures. (**e**) Sagittal MIP with contrast proximal to occlusion highlighted (*arrow*). (**f**) Axial image showing R popliteal artery with normal enhancement (*green arrow*) as compared to diseased L popliteal artery (*white arrow*)

single breath-hold is necessary (during abdominal acquisitions), and scan times can be as short as 15–40 s. The entire study can involve less than 15 min of room time, making CTA useful when rapid assessment of critical limb ischemia is required, as opposed to more time-consuming modalities such as ultrasound or MRI. Table 17.2 contains a CTA runoff

Table 17.1 Key terms

Pitch	Table feed per rotation in a spiral scan divided by the total width of the collimated beam. Pitch, $p < 1$ signifies data acquisition with overlap in the longitudinal direction
Gantry rotation	The gantry is the spherical portion of the CT that houses the X-ray tube and the detector. One gantry rotation is one 360-degree rotation around the patient over a period of time
Voxel	Each CT image has a defined thickness. The smallest distinguishable matrix in a CT image is known as voxel, which is a pixel with a defined thickness
Attenuation	The loss of X-ray beam strength as it passes through an object. Usually highly attenuating structures are denser, making it harder for X-rays to pass through, allowing for stronger reflection and brighter appearance on CT imaging
Dual-source CT	Makes use of two X-ray and detector sources perpendicular to each other. This increases temporal resolution, reduces radiation, and increases the speed of image acquisition
Kernels	Post-processing filter or algorithm applied to the raw CT images to specifically select for desired structures. For example, a "sharper" kernel will increase the image contrast but will also introduce more noise
Hounsfield Unit	A unit of measurement to quantify radiodensity. A more radiopaque structure has a higher value. A HU of 0 is calibrated to the radiodensity of distilled water at standard pressure and temperature (STP)
Detector rows	The area across from the X-ray beam within the gantry. It receives the X-ray beam after it passes through an object. Multiple detector rows allow the acquisition of images from slightly different angles resulting in greater volume coverage and scan speed

protocol utilized at Loyola University Medical Center, adopted from D. Fleischmann at Stanford University.

Basic Principles of Image Acquisition

The scout image is typically a coronal topogram from below the diaphragm (to include the renal arteries) to the tip of the feet, roughly 130 cm. Contrast is injected through an established peripheral IV typically no smaller than 20G. The amount of time needed for contrast to appear in the abdominal aorta, the contrast transit time, can be accounted for via test bolus or bolus-triggering protocols. This is important as it determines when to start image acquisition. For bolus triggering, a region of interest is identified in the abdominal aorta typically at a level above the renal arteries, and an attenuation threshold is set (e.g., 130 HU). The scan is started when a desired attenuating threshold is met. A test bolus (typically 20 cc) can allow for correct timing of scan initiation; however, table speed and overall scan times should be carefully selected as to not allow image acquisition to "outrun" the contrast. Low flow states, such as with cardiomyopathy, and severe atherosclerotic disease should be accounted for. Additionally, aortic aneurysms can have turbulent blood flow with dilution of contrast media and cause delay in transit. Another approach is to calculate aortic and popliteal transit times via the use of two test boluses. Of note, prolonged scan times may also result in venous opacification, which can be adjusted for in post-processing. Contrast flow

Fig. 17.2 A 65-year-old male with known peripheral arterial disease, with a history of acute-on-chronic left lower extremity claudication, found to have stenosis of the right superficial femoral artery. (**a**) Magnified CTA-MIP showing severe stenosis of SFA mid-thigh with atherosclerotic plaque along its course. (**b**) DSA showing the same SFA stenosis
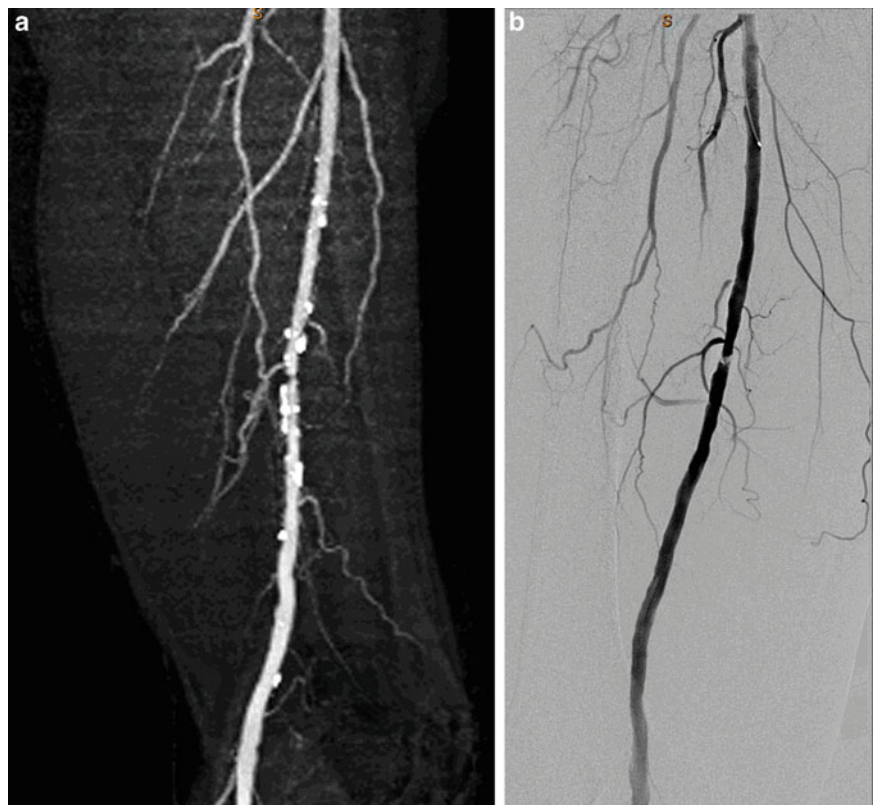
Fig. 17.3 A 65-year-old male with HTN, DM, HLD presenting with LLE claudication and L common iliac stenosis. (**a**) CTA-MIP showing calcified plaque causing high-grade stenosis at the origin of L common iliac artery (*inferior arrow*). Also, note the presence of mural thrombus with calcification (*superior arrow*) in the distal abdominal aorta just above the bifurcation. (**b**) DSA demonstrating the same severe L common iliac stenosis (*arrow*)
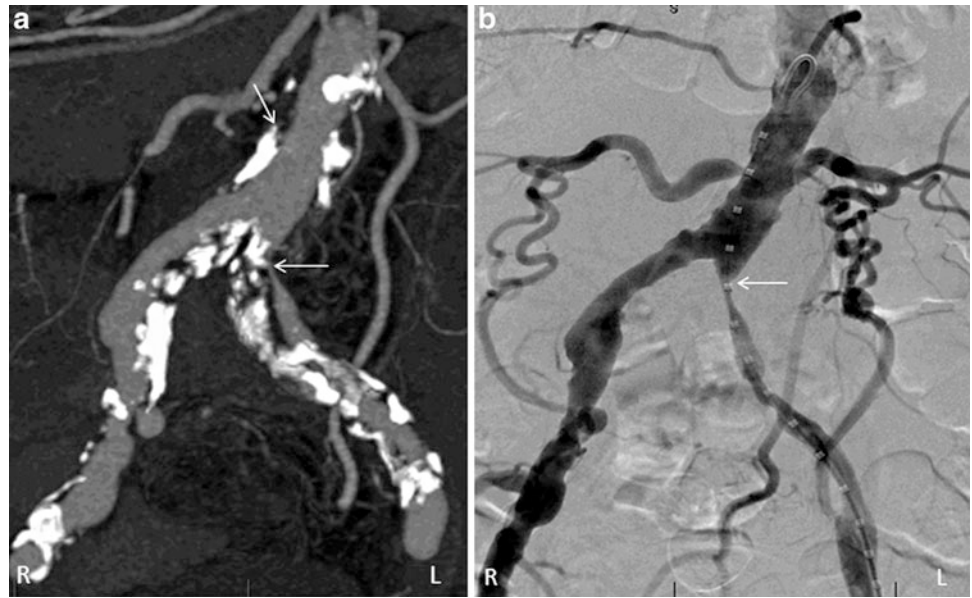

Fig. 17.4 A 58-year-old heavy smoker, who presents with LLE pain, found to have a popliteal aneurysm containing thrombus. (**a**) Full MIP showing bilateral fem-pop circulation with L popliteal aneurysm (starred). (**b**) MPR-left sagittal view of popliteal aneurysm with thrombus. (**c**) MPR-axial images of the left popliteal aneurysm. Note the normal right popliteal artery for comparison in axial view. *Arrows* in b and c outline the aneurysm containing thrombus
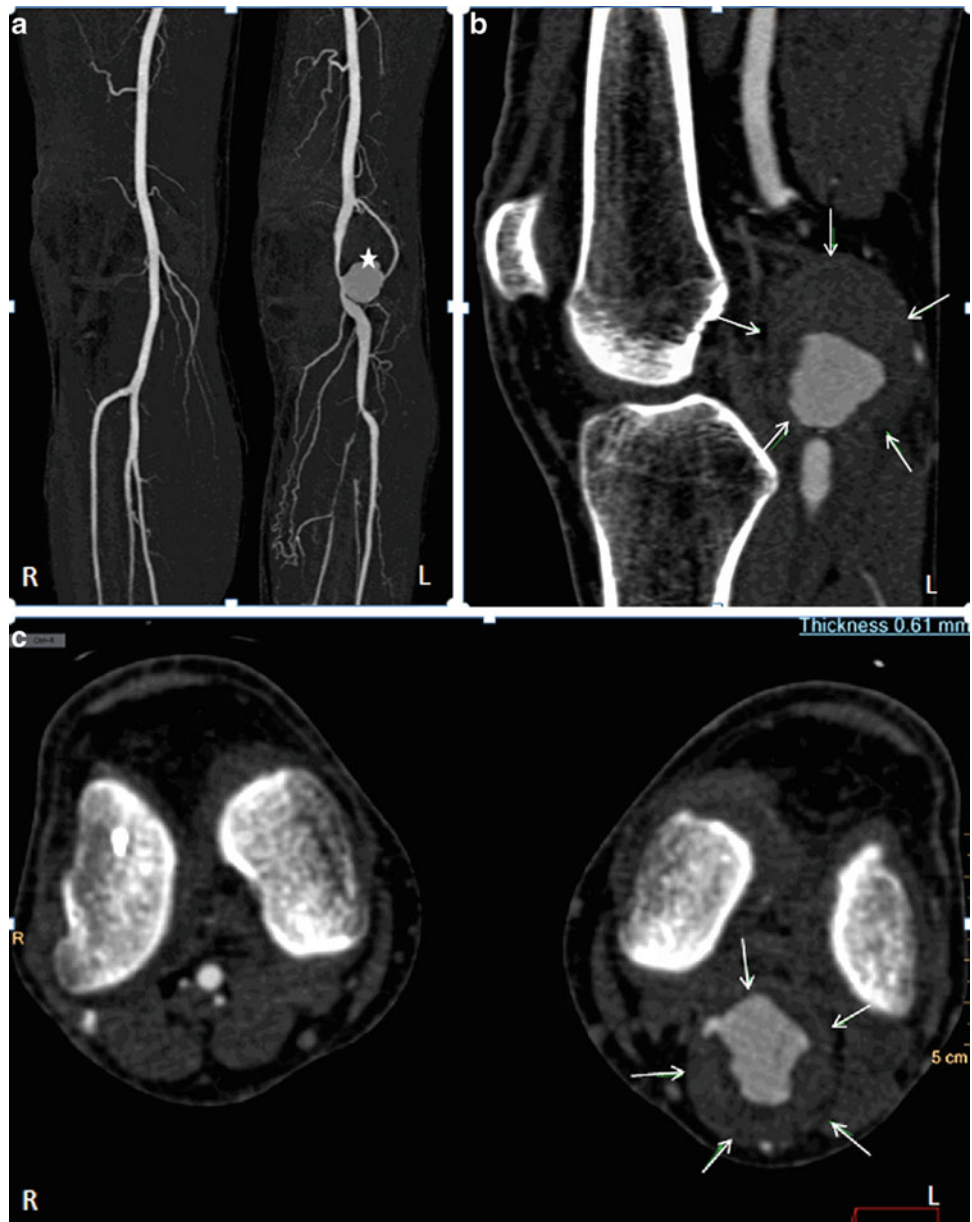
Table 17.2 Scanning protocol; adapted from D. Fleischmann, Stanford University Medical Center

Lower extremity runoff, Siemens S 64	
Topogram	1500 mm AP; feet first, arms up; feet still and relaxed; support with cushions/tape
Range 1 + 2	Bolus tracking, ROI in the abdominal aorta at the level of the celiac artery
Range 3	Runoff: from above the celiac trunk (D12 vertebral body) through the toes 120 kV/Care dose 4D w. 250 ref-mAs (voltage weight adjusted)
	64 × 0.6 mm, 0.5 s gantry rotation
	40 s scan time (will result in a pitch <1)
	Set scan range first and then change scan time to 40 s
Range 4	Runoff: Preprogrammed optional second CTA acquisition to cover popliteal and crural territories. This range is only initiated if there is no contrast medium opacification seen in the popliteal/crural vascular territories
Breath-hold	At inspiration
Scan direction	Cranio-caudal
Injection	20–22G IV line, Isovue (iopamidol) 370
Protocol	Bolus tracking with ROI in the abdominal aorta (beginning of scan range)
	Minimum delay (3 s including automated breath-hold command)
	Use biphasic injection protocol with 35 s injection duration
	Injection rates and volumes (adjusted to patient size)

	Weight (kg)	Vol1 (mL)	Flow1 (mL/s)	Vol2 (mL)	Flow2 (mL/s)
XS	<55	20	4	96	3.2
S	<65	23	4.5	108	3.6
Avg	75	25	5	120	4
L	>85	28	5.5	132	4.4
XL	>95	30	6	144	4.8
	Saline flush: 40 mL volume, flow rate equal to "Flow2"				

Reconstruction (STh/RI)	
Range 3	2/1.0, B25f (patients w. Fontaine IIb)
	1/0.7, B25f (patients w. Fontaine III/IV)
	5/5, B31f Abd/Pel only
Range 4	1/0.7, B25f

rate and volume can be adjusted for body weight/size and delivered via a power injector. Typical flow rates are between 3 and 6 mL/s of iodinated contrast media, resulting in approximately 1.5 g of iodine per second depending on media concentration selected and total contrast volume around 130 mL. Biphasic injections are often used to provide steady delivery over time.

Radiation Exposure

Tube voltage, collimation, and pitch can be adjusted to reduce radiation exposure and maintain adequate resolution, with lower voltage for patients with lower BMI. Protocols have been developed lowering the tube voltage from commonly used 120–80 kVp, showing significant reductions in radiation exposure [5]. Using a 64 channel multi-detector CT, Iezzi et al. demonstrated a weighted CT dose index of 12.96 mGy for their 120-kVp moderate noise reduction protocol, 6.34 mGy for their 80-kVp moderate noise reduction protocol, and 5.89 mGy for their 80-kVp high noise reduction protocol, with an effective calculated dose of 29.32, 14.64, and 11.43 mSv, respectively. These protocols combined with

a high iodine concentration media allowed for significant radiation reduction, up to 61 %, without sacrificing image quality. Low radiation doses and good diagnostic performance have also recently been demonstrated with 128 slice dual-source CT using 80 kVp with high pitch [6]. For a point of reference, a chest X-ray gives a radiation dose of 0.01 mSv, and annual background radiation is 3.0 mSv [1]. Preserving scan quality with decreasing radiation remains an active area of research.

Post-processing Techniques

Post-processing techniques have dramatically advanced our ability to detect steno-occlusive disease, aiding in identification of lesion severity, length, and number along the course of any given vessel. Stacks of two-dimensional axial slices can be assimilated into three-dimensional volumetric data sets. From these data sets, maximum intensity projections (MIPs), multiplanar reformatted (MPR) images, curved multiplanar (CPR) images, and volume-rendered images can be created to aid in pathological analysis (Fig. 17.5). A maximal intensity projection (MIP) provides a layout that most

Fig. 17.5 A 50-year-old female with known PAD and RLE claudication, found to have severe right SFA stenosis with collateralization. (**a**) and (**b**) show VR images with transparent bone and bone removed, respectively, that help visualize the vasculature in relation to adjacent structures. (**c**) Coronal CPR of R SFA highlighting atherosclerotic disease (*arrow*). (**d**) MIP showing diseased R SFA (*white arrows*) and well-developed collateralization via the deep femoral artery (*yellow arrows*). (**e**) VR with transparent bone showing extent of vasculature to pedal arteries (*arrow*)

closely resembles an invasive angiogram and is very useful in providing a road map view of the course of peripheral vessels. MIPs are created by displaying the brightest voxel in every ray or line of sight. This ensures that high attenuation structures such as contrast-filled vessels and calcification/bone are prominently displayed. The bone is typically removed by automated or semiautomated programs, leaving the arterial tree. One should be aware that this can be a source of artifact (editing misregistration, Fig. 17.6). MIPs however do not provide adequate depth information and can pose a problem defining relationships to anatomic structures. Volume-rendered images however provide color and three-dimensional displays of the vasculature in relation to organs and bone, which can additionally be edited. The MIP and VR image alone is not sufficient for evaluating vessel stenosis in the presence of dense calcifications or stents, because the brightness of these elements can obscure interpretation of the vessel lumen. Thin-slab MIPs and multiplanar reformations allow better visualization of steno-occlusive disease in the presence of calcifications and stents (Fig. 17.7). The most basic MPRs are transverse cuts such as sagittal and coronal images. However, because peripheral vessels can be tortuous, they may cut in and out of the MPR plane, thus allowing only short segments of the vessel of interest to be

Fig. 17.6 Editing artifact secondary to bone removal misregistration, leading to inadvertent removal of adjacent vasculature (*arrows*)

viewed. In this case, the vessel path can be traced along its center line using multiple MPR (coronal, sagittal, oblique) and axial images to create a curved planar reformatted image (CPR) which can delineate an entire vessel's course, in one image. CPR images are essential in evaluating eccentric lesions, since multiple cross-sectional views are obtained to adequately visualize the vessel lumen and construct the CPR image. MPR/CPR slices can be thickened as needed for full vessel view.

Imaging Artifacts

With calcifications, endovascular stents and automated image processing, certain artifacts, and misrepresentations may arise, which are summarized in Table 17.3. In the setting of a narrow viewing window, calcifications or stent struts can display overly bright and appear artificially larger in size giving the appearance of more severe steno-occlusive disease and thus overestimation of disease severity. This is known as blooming artifact (Fig. 17.8). Window level/width should be increased for better grayscale differentiation to diminish brightness of calcification/stents and allow visualization of vessel lumen when possible. Editing artifacts, perhaps during automated bone removal, may lead to false vessel narrowing or occlusion if part of the vessel is misreg-

istered and removed as the bone. Alternatively, misregistration can cause part of the bone to be left in mimicking pathological disease. Stents can also provide streak artifacts known as beam hardening. Multiple view MPR and CPR images are paramount for further analysis. However, inaccurately drawn center lines when constructing CPR images can overestimate steno-occlusive disease.

CTA Evaluation of Vascular Stents

Stent evaluation has made progress in the era of 64 slice multi-detector CT scanning with improved resolution and image reconstruction. Despite this, there are still challenges, such as metallic (gold) markers at bilateral stent edges providing artifact that can hinder interpretation [7]. When stents are overlapped, the artifact can extend to the stent body. In a study using 64 slice MDCT to evaluate 41 patients with a total of 81 stents, Li et al. found that 19 stents (23.5%) had uninterpretable segments due to artifact. Protocol parameters included collimation width 64 mm × 0.6 mm, pitch 1.1, rotation time 0.33 s, table speed 63 mm/s, tube voltage 120 kV, and tube current 250 mAs. They determined that specificity remained high despite sensitivity being somewhat lower due to un-evaluable stents and concluded that overall accuracy for detecting in-stent stenosis was still acceptably good [7]. Multiple cross-sectional views using multiplanar reformatted images should be used for stent lumen evaluation. Furthermore, contrast enhancement of distal runoff vessels alone was found not to be a reliable indicator of stent patency, due to the presence of collateral vessels. Collateralization can be well appreciated by CT angiography (Fig. 17.9).

In order to evaluate stent restenosis, not only must one visualize the lack of contrast within the lumen in a sagittal or coronal section but also look at specific axial sections to truly evaluate stent patency. Manipulation of raw CTA is needed to help enhance spatial resolution. Spatial resolution can be improved by decreasing slice thickness and by manipulating reconstruction kernels or filters.

Kohler et al. used dual-source CT (DSCT) to evaluate stent characteristics by analyzing lumen diameter, intraluminal density, and noise of 22 peripheral stents in a vessel phantom [8]. The vessel phantoms that were used were made of plastic tubes of different diameters filled with contrast material and then submersed in vegetable oil diluted to 250 HU and then in a larger plastic container, which was then diluted to −70 HU to simulate perivascular fat. Each of the 22 stents of different luminal size and length then underwent DSCT with four different types of image acquisitions that were obtained by different reconstruction kernels. It was found that visualized stent lumen diameter varied depending on the type of stents. Visibility of the lumen diameter could

Fig. 17.7 A 64-year-old female with history of PAD status-post RLE bypass, presenting with LE ischemic pain found to have left common iliac stent stenosis. (**a**) DSA with selective engagement of the L iliac artery showing in-stent stenosis. (**b**) CTA-MIP reveals in-stent stenosis (*arrows*). (**c**) Sagittal CPR and (**d**) coronal CPR are used to delineate vessel course along with stenotic disease (*arrows*)
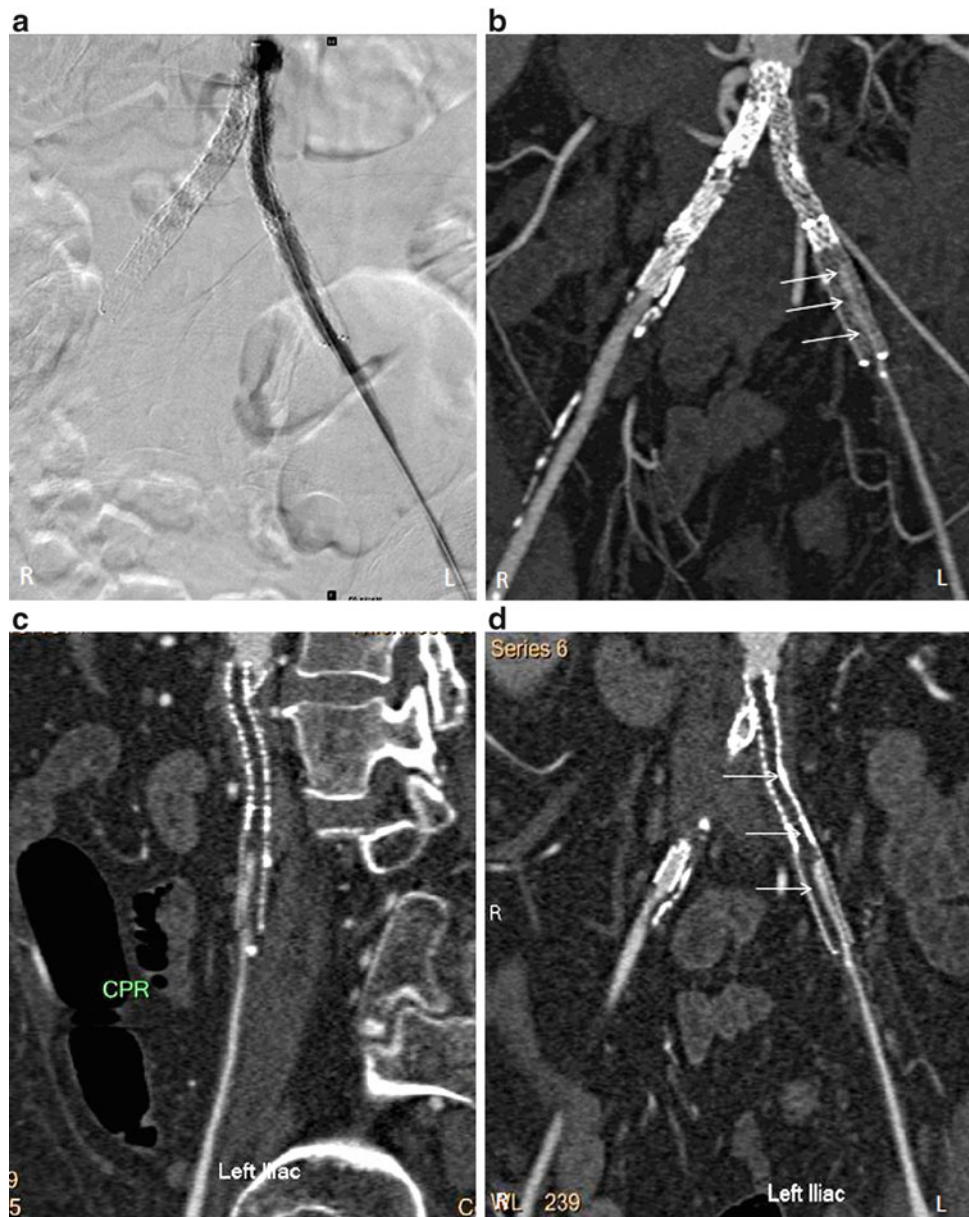

Table 17.3 Common artifacts [13]

| Beam hardening	Artificial darkening of the center of an object compared to its edges. This happens secondary to the polychromatic nature of the X-ray beam with different attenuation rates as it passes through an object
Blooming	This artifact is caused by the CT software's averaging of signal intensity from a given imaging region. This is common to see in images with high-attenuating structures adjacent to low attenuating structures. For example, vessel stenosis severity may be overestimated secondary to blooming from adjacent calcified plaque
Streaking	Dark streaks that appear between highly attenuating structures. It can be reduced by increasing the kV of the X-ray, with risk of compromising the contrast of the image
Cone beam artifact	With MDCT, the X-ray beam is detected at an angle from the individual detector source. Thus if there is a high contrast edge, it can lead to dark streaks on the image
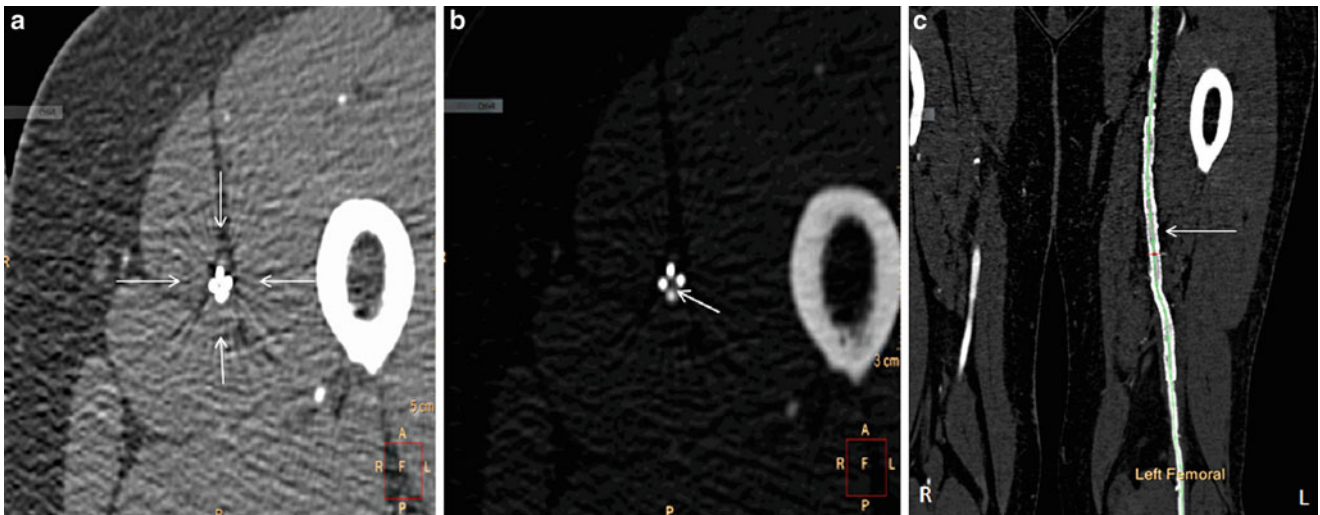
Fig. 17.8 (**a**) Cross-sectional image of a femoral stent shows streaking artifact (radial lines emanating from the center) and blooming artifact (inappropriate radiodensity of stent struts leading to concealment of vessel lumen). (**b**) Blooming artifact reduced by manual changes in window/level allows for the vessel lumen to be visualized (*arrow*). (**c**) Femoral stent in a and b, in curved planar reconstruction, providing visualization of the lumen throughout the vessel's course. The *green line* represents the constructed "center line." Arrow approximates the half-way point of the femoral stent

Fig. 17.9 A 53-year-old patient with history of bilateral lower extremity PAD status-post L fem-peroneal bypass and multiple peripheral stents, with bilateral femoral stent occlusion and patent LLE bypass graft (*green arrow*) and patent RLE collaterals. (**a**) MPR image showing bilateral stents that are occluded (*arrows*). (**b**) 3D MIP showing the patency of LLE bypass graft (*green arrow*) and RLE collateral vessels (*white arrow*) which provide adequate distal flow in the setting of occluded femoral stents
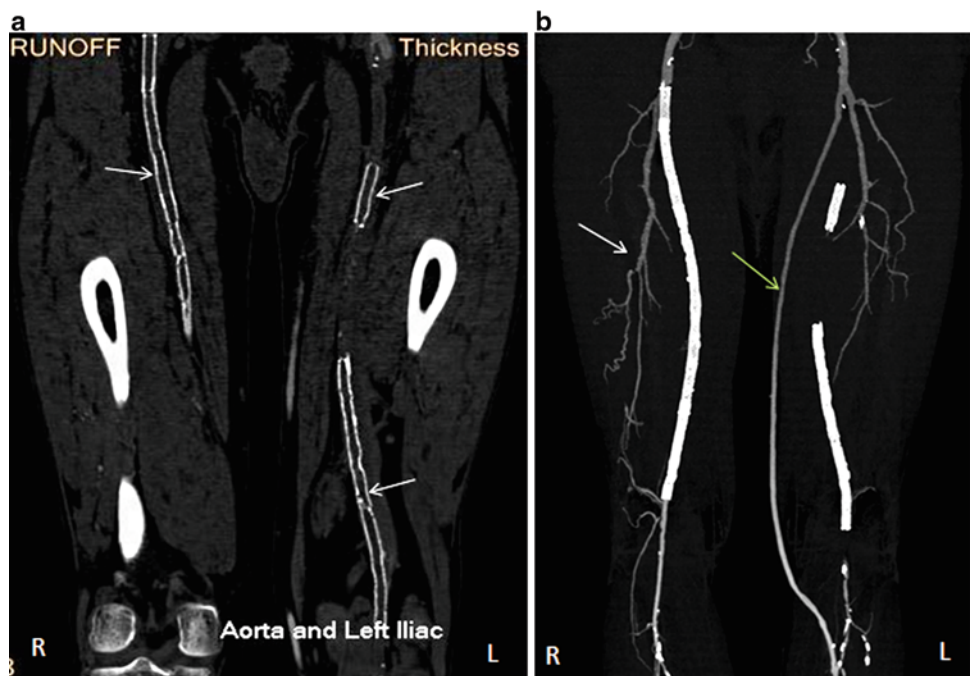
Fig. 17.10 An example of the level of detail of the infra-popliteal system that can be achieved by CTA with distal runoff and bolus tracking

be increased with increasing the sharpness of reconstruction kernel, whereas smoothening of the reconstruction kernel resulted in more realistic intraluminal density measurement with less intraluminal noise. It is important to note that while assessing for stent restenosis, the CTA protocol may need to be tailored based on the type of stent being evaluated [8].

Imaging of Infra-popliteal Vasculature

In patients with extensive arterial wall calcification or atherosclerosis, imaging of infra-iliac and specifically infra-popliteal arteries can be difficult due to slower flow of contrast through these areas and resulting CT image acquisition "outrunning" the contrast. To compensate, a test run is done from below the diaphragm to the toes. Next, the delay time between the initiation of contrast administration and the initiation of scanning for optimal intraluminal contrast enhancement is calculated. Those with poor cardiac output or slow

distal runoffs can undergo delayed imaging, for example, 90 s delay from contrast initiation. This technique is not always necessary and should only be employed when the poor enhancement of the distal arteries is noticed after the initial scan (Fig. 17.10).

Digital Subtraction Angiography (DSA) and CTA

Although DSA is used as a reference standard against which noninvasive imaging is compared, it has downsides as well, one limitation being two-dimensional imaging of a three-dimensional structure. The severity of an occlusion may be over- or underestimated depending on the angle from which the vessel's image is acquired [9]. In a study comparing pre-amputation angiogram vs. post-amputation pathology, DSA tended to underestimate the severity of stenosis, plaque concentricity, and grading of calcification even in normal-
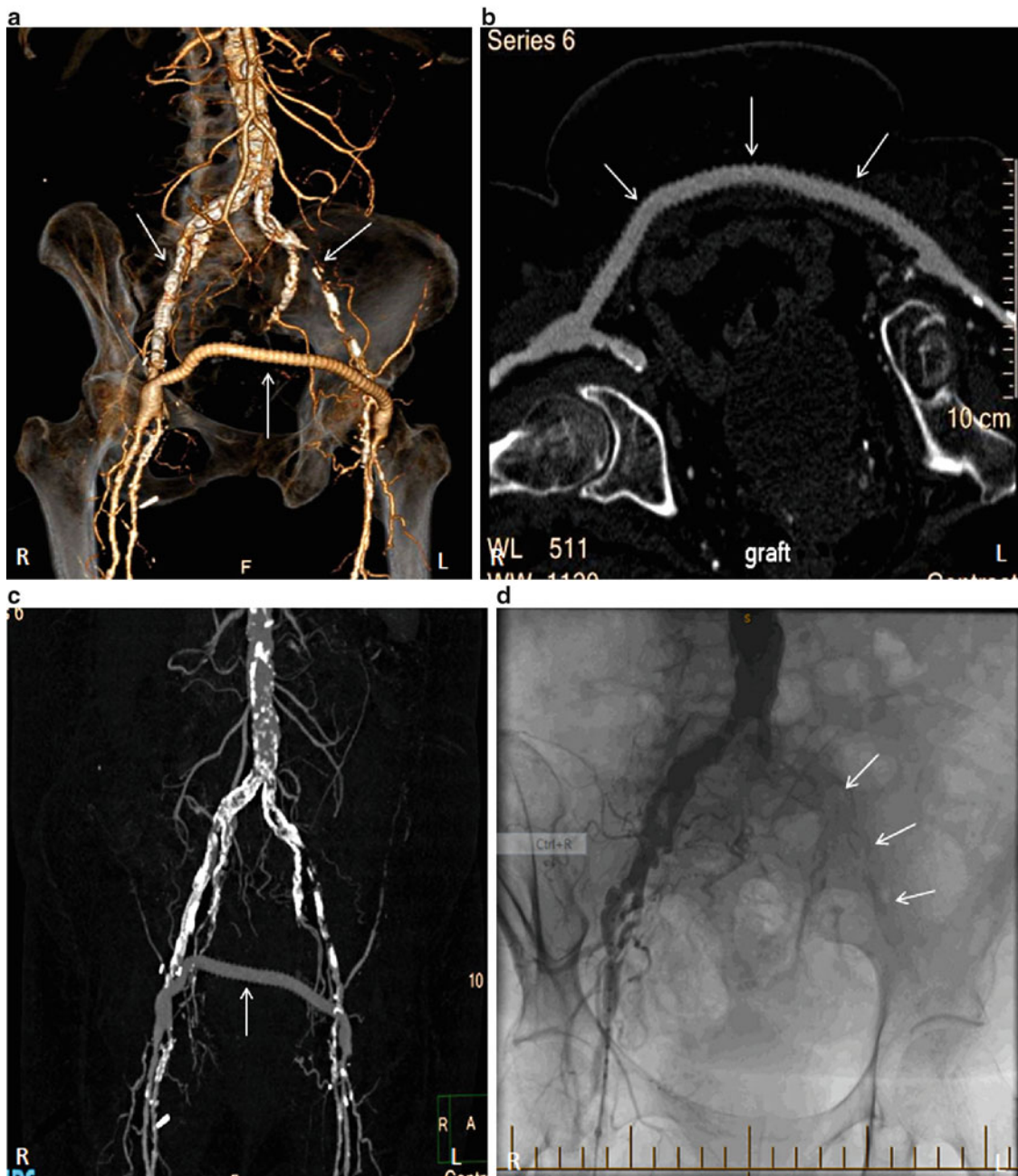
Fig. 17.11 A 68-year-old female with CAD status-post CABG, ESRD, DM who underwent fem-fem bypass grafting after DSA revealed occluded L iliac artery. (**a**) 3D VR shows severe steno-occlusive disease of the left iliac artery (*superior arrows* depict L and R external iliac arteries, *inferior arrow* depicts bypass graft). (**b**) CPR showing patency of the fem-fem bypass graft. (**c**) 3D full MIP again showing calcified atherosclerotic disease burden with patent fem-fem bypass graft (*arrow*). (**d**) DSA performed pre-bypass grafting showing occlusion of the L iliac artery

appearing vessels [10]. Another drawback is DSA's need for good contrast timing for visualization of the vasculature in satisfactory detail. This task may be difficult in assessing different bypass grafts given complex anatomy leading to poor contrast timing and suboptimal vessel opacification (Fig. 17.11). Compared with conventional DSA, the sensitivity and specificity of multi-detector row CT (MDCT) angiography in the detection of significant stenosis, aneurysmal changes, and arteriovenous fistulas of arterial bypass grafts were more than 95 % [11] (Fig. 17.12). Advances in MDCT and post-processing techniques make CT angiography a valuable tool in the assessment of critical limb ischemia, acute and chronic [12].

Fig. 17.12 A 28-year-old male with history significant for a gunshot wound to his RLE, status-post fempopliteal bypass, who presents with LE pain. (**a**) CTA-MIP showing femoral-popliteal bypass (*arrow*) and its distal touchdown site. (**b**) DSA in comparison. Note the similar angiographic findings

References

1. Met R, et al. Diagnostic performance of computed tomography angiography in peripheral arterial disease. A systematic review and meta-analysis. JAMA. 2009;301(4):415–24.
2. Schernthaner R, et al. Multidetector CT angiography in the assessment of peripheral arterial occlusive disease: accuracy in detecting the severity, number, and length of stenosis. Eur Radiol. 2008;18:665–71.
3. Napoli A, et al. Peripheral arterial occlusive disease: diagnostic performance and effect on therapeutic management of 64-section CT angiography. Radiology. 2011;261(3):976–86.
4. Fotiadis N, et al. 64-section CT angiography in patients with critical limb ischemia and severe claudication: comparison with digital subtractive angiography. Clin Radiol. 2011;66:945–52.
5. Iezzi R, Santoro M, Marano R, Di Stasi C, Dattesi R, Kirchin M, Tinelli G, Snider F, Bonomo L. Low-dose multidetector CT angiography in the evaluation of infrarenal aorta and peripheral arterial occlusive disease. Radiology. 2012;263(1):287–98. doi:10.1148/radiol.11110700.
6. K.S. Choo, et al. Diagnostic performance and radiation dose of lower extremity CT angiography with 128-slice dual source CT using 80 kVp plus high pitch. ECR. 2014;Poster C-1372.
7. Li XM, et al. Evaluation of peripheral artery stent with 64-slice multi-detector row CT angiography: prospective comparison with digital subtraction angiography. Eur J Radiol. 2010;75:98–103.
8. Kohler M, et al. Dual-source CT angiography of peripheral arterial stents: in vitro evaluation of 22 different stent types. Radiol Res Pract. 2011;2011: Article ID 103873, 7 p. doi:10.1155/2011/103873.
9. Duran C, Bismuth J. Advanced imaging in limb salvage. Methodist Debakey Cardiovasc J. 2012;8:28–34.
10. Kashyap VS, Pavkov ML, Bishop PD, et al. Angiography underestimates peripheral atherosclerosis: lumenography revisited. J Endovasc Ther. 2008;15(1):117–25. doi:10.1583/07-2249R.1.
11. Willmann JK, Mayer D, Banyai M, Desbiolles LM, Verdun FR, Seifert B, Marincek B, Weishaupt D. Evaluation of peripheral arterial bypass grafts with multi–detector row CT angiography: comparison with duplex US and digital subtraction angiography. Radiology. 2003;229(2):465–74.
12. Fleischmann D, Hallett RL, Rubin GD. CT angiography of peripheral arterial disease. J Vasc Interv Radiol. 2006;17(1):3–26. Review.
13. Boas E, Fleischmann D. CT artifacts: Causes and reduction techniques. Imaging Med. 2012;4(2):229–40. http://www.edboas.com/science/CT/0012.pdf.